

## FAST COMMUNICATIONS

Contributions intended for this section should be submitted to any of the Co-editors of the *Journal of Applied Crystallography*. In the letter accompanying the submission, authors should state why rapid publication is essential. The paper should not exceed two printed pages (about 2000 words or eight pages of double-spaced typescript including tables and figures) and figures should be clearly lettered. If the paper is available on a 3.5 or 5.25 in IBM PC compatible or 3.5 in Apple Macintosh diskette, this should be sent with the manuscript together with details of the word-processing package used. Papers not judged suitable for this section will be considered for publication in the appropriate section of the *Journal of Applied Crystallography*.

*J. Appl. Cryst.* (1996). **29**, 608–613

### A simple device for studying macromolecular crystals under moderate gas pressures (0.1–10 MPa)

MICHAEL H. B. STOWELL,<sup>a\*</sup> S. MICHAEL SOLTIS,<sup>b\*</sup> CAROLINE KISKER,<sup>a</sup> JOHN W. PETERS,<sup>a</sup> HERMANN SCHINDELIN,<sup>a</sup> D. C. REES,<sup>a</sup> DUILIO CASCIO,<sup>c</sup> LESA BEAMER,<sup>c</sup> P. JOHN HART,<sup>c</sup> MICHAEL C. WIENER<sup>d</sup> AND FRANK G. WHITBY<sup>e</sup> at <sup>a</sup>Division of Chemistry and Chemical Engineering, Mail Stop 147–75CH, California Institute of Technology, Pasadena CA 91125, USA, <sup>b</sup>Stanford Synchrotron Radiation Laboratory, SLAC, PO Box 4349, Bin 69, Stanford University, CA 94309, USA, <sup>c</sup>Molecular Biology Institute, UCLA-DOE LSBMM, Department of Chemistry and Biochemistry, University of California Los Angeles, Los Angeles CA 90024, USA, <sup>d</sup>Department of Biochemistry and Biophysics, University of California San Francisco, San Francisco CA 94143, USA, and <sup>e</sup>University of Utah Medical Center, Department of Biochemistry, 50 North Medical Drive, Salt Lake City UT 84132, USA.  
E-mail: stowell@citray.caltech.edu

(Received 12 December 1995; accepted 9 April 1996)

#### Abstract

A simple device for studying crystalline samples under moderate gas pressure (0.1–10 MPa) has been developed. The device employs a modified Cajon ultra-torr fitting to ensure a gas-tight seal around an X-ray capillary. The cell accommodates standard X-ray capillaries that require no modification. The device is straightforward to utilize and samples can be mounted with routine techniques and pressurized in a matter of seconds. In a subsequent development, a complete purging and pressurization system has been designed and constructed for use on beamline 7-1 at the Stanford Synchrotron Radiation Laboratory. This paper describes the construction of both the pressure cell and the delivery system and presents results of the use of this cell for the preparation of xenon derivatives to be used in phase determination by the multiple isomorphous replacement method.

#### 1. Introduction

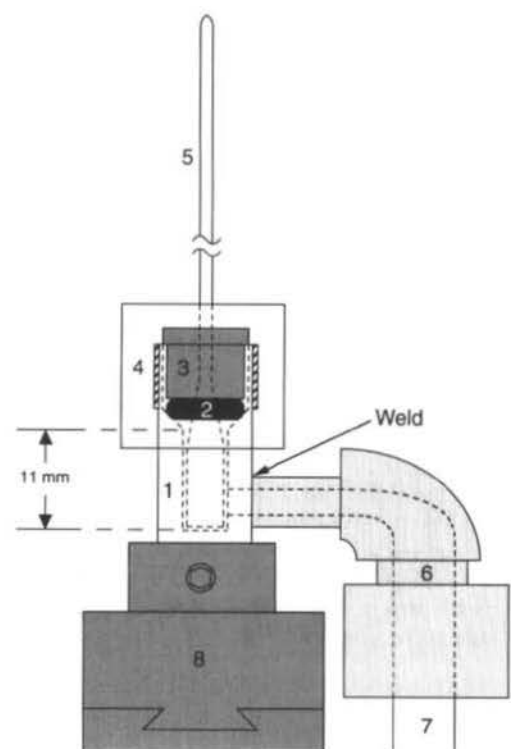
The incubation of macromolecular crystals with gases, to study ligand binding or for the preparation of xenon heavy-atom derivatives, has prompted the development of suitable cells and mounting techniques (Schoenborn, Watson & Kendrew, 1965; Tilton, Kuntz & Petsko, 1984; Kroeger & Kundrot, 1994; Schiltz, Prange & Fourme, 1994). Here, we report the development of a simple device for mounting and studying protein crystals under moderate gas pressures in the range 0.1–10 MPa in a routine manner. This pressure cell has a distinct advantage over previously reported devices in that it can accommodate standard-sized closed-end X-ray capillaries up to 1.5 mm in diameter without modification. In addition, standard crystal-mounting techniques can be employed and a mounted crystal can be quickly placed in the cell and studied at a desired pressure. The pressure cell is straightforward to employ and has been successfully used by a number of experimenters, many of whom were only briefly instructed in its operation. The original device was constructed for use on an *R*-axis IIC imaging-plate

system and utilizes a low-profile design necessary for the limited goniometer *z* translation of this instrument. A standard cell has also been designed and fabricated that can be mounted on a standard Huber goniometer head. In a subsequent implementation, a safe and simple-to-use purge and pressurization system has been designed and constructed for use on beamline 7-1 at the Stanford Synchrotron Radiation Laboratory (SSRL).

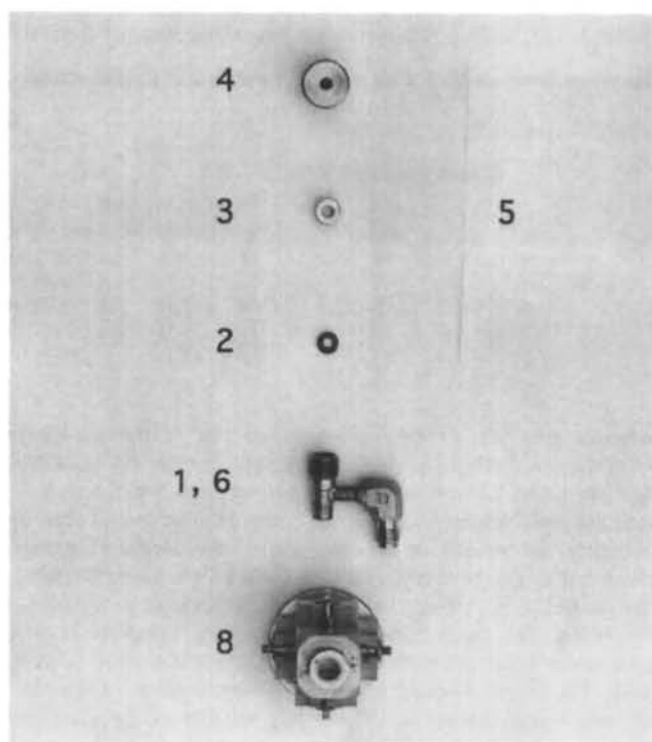
We have attempted to prepare xenon derivatives of nine different protein crystals, using pressures from 0.4 to 2 MPa. The results of these trials range from excellent derivatives to extreme nonisomorphous crystals. Of the nine proteins studied, five gave xenon derivatives with useful phasing information, two gave poor results, indicating weak or no binding, and two were nonisomorphous. Several conclusions from these studies can be drawn: In general, the xenon binding site(s) are different from other heavy-atom sites. Xenon derivatives can be highly isomorphous; however, nonisomorphism does occur and appears to be a consequence of xenon binding, not of pressure effects or xenon hydrate formation. The ease and success of xenon-derivative preparation suggests that xenon should be used in a standard derivative screen for any newly crystallized protein of which the structure is to be determined by multiple isomorphous replacement (MIR) methods.

#### 2. Pressure cell design

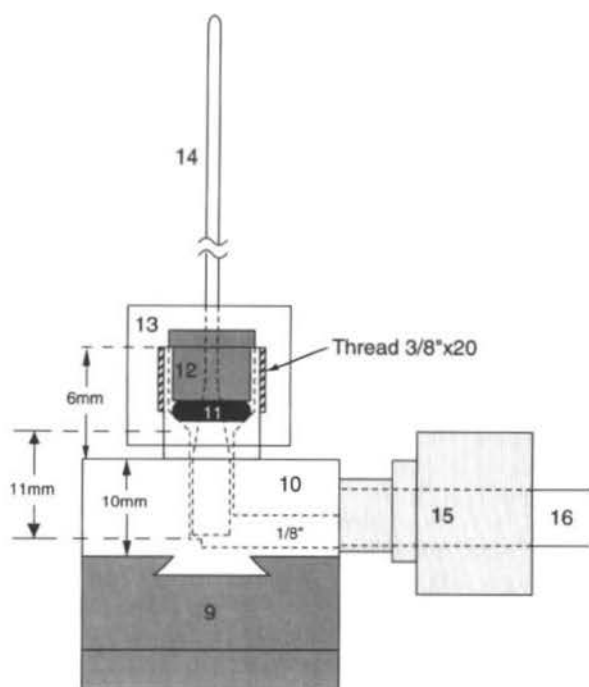
Two gas pressure cells were designed for use on two different area-detector systems. A schematic diagram of the standard pressure cell is shown in Fig. 1(a), with an exploded-view photograph of the actual cell shown in Fig. 1(b). The numbers in parentheses refer to individual components shown in Fig. 1. This cell is composed primarily of a standard  $\frac{1}{8}$  in (~0.3 cm) Cajon ultra-torr fitting (1, 2, 3 and 4) (Sunnyvale Valve and Fitting Company, Sunnyvale, CA, USA) that has been slightly modified to accommodate X-ray capillaries (5) (Charles Supper Company, Natick, MA, USA). The body (1) has been modified by an increase of the depth of the central bore to 11 mm, thus



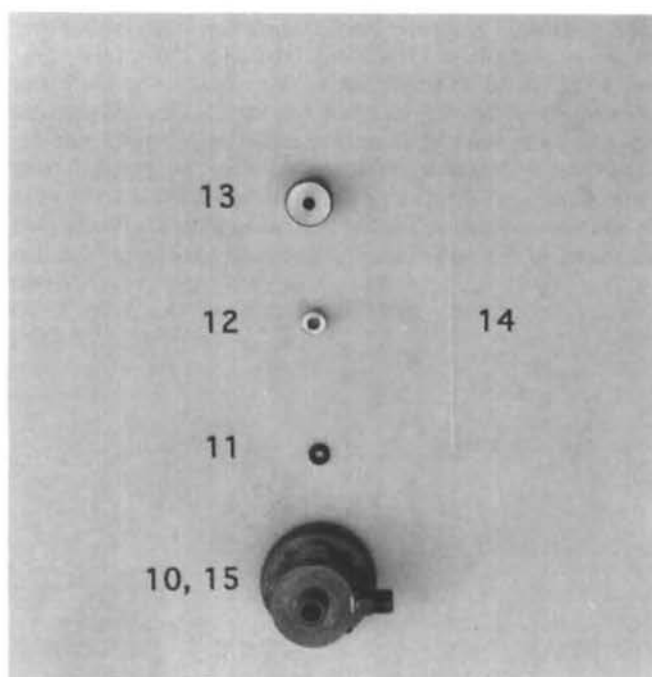
(a)



(b)



(c)



(d)

Fig. 1. Schematic diagrams and exploded-view photographs of the components of the standard [(a) and (b)] and low-profile [(c) and (d)] pressure cells. The numbers are shown in parentheses in the text. 1  $\frac{1}{8}$  in Ultra-torr fitting body; 2 O ring; 3 grommet; 4 tightening cap; 5 X-ray capillary; 6  $\frac{1}{8}$  in Swagelok elbow fitting; 7  $\frac{3}{8}$  in flexible Teflon tubing; 8 goniometer head; 9 goniometer head; 10 integral body and goniometer slide; 11 O ring; 12 grommet; 13 cap; 14 X-ray capillary; 15  $\frac{1}{8}$  in Swagelok elbow fitting; 16  $\frac{1}{8}$  in flexible Teflon tubing.



Table 1.  $I/I_0$  values (%) for xenon pressures ranging from 0.1 to 15 MPa and capillary diameters ranging from 0.1 to 1.0 mm. The values listed are for Cu  $K\alpha$  and 1.0 Å wavelength (in parentheses) X-rays.

Xenon pressure (MPa)	Capillary diameter (mm)					
	0.1	0.2	0.3	0.5	0.7	1.0
0.1	98.4 (99.5)	96.8 (98.9)	95.3 (98.5)	92.2 (97.5)	89.2 (96.5)	85.1 (95.0)
0.5	92.2 (97.5)	85.1 (95.0)	78.4 (92.6)	66.7 (87.9)	79.7 (83.5)	44.5 (77.3)
1	85.1 (95.0)	72.3 (90.2)	61.5 (85.7)	44.5 (77.3)	32.2 (69.7)	19.8 (59.7)
2	72.3 (90.2)	52.3 (81.4)	37.7 (73.4)	19.8 (59.7)	<0.1 (48.6)	<0.1 (35.7)
5	44.5 (77.3)	9.8 (59.7)	<0.1 (46.1)	<0.1 (27.5)	(<0.1)	(<0.1)
10	19.8 (59.7)	<0.1 (35.6)	(21.3)	(<0.1)		
15	<0.1 (46.1)	(21.3)	(<0.1)			

ensuring that the  $O$  ring (2) seal occurs at the capillary constriction (see Fig. 1*a*). With this design feature, any standard capillary up to 1.5 mm in diameter can be placed in the cell. A standard  $\frac{1}{8}$  in Swagelok fitting (6) (Sunnyvale Valve and Fitting Company) is welded on to the side of the ultra-torr fitting connected to a flexible high-pressure Teflon PFA tube (7) (Cole-Parmer, Niles, IL, USA). The diameter of the base of the ultra-torr fitting has been reduced to fit into a standard Huber goniometer head (8) (USA source: Blake Industries, Scotch Plains, NJ, USA). Another important design feature is the small size and compactness that allows full rotation of the pressure cell on most data-collection systems.

The original cell was designed for use on area detectors that have a limited goniometer  $z$  translation, e.g. the  $R$ -axis IIC or MAC Science imaging-plate detector systems. A schematic diagram of the low-profile pressure cell, required for X-ray data-collection systems with space constraints, is shown in Fig. 1*c*, with an exploded view of the actual cell shown in Fig. 1*d*. A standard Huber or Enraf-Nonius top-arc goniometer (9) serves as the base for this cell. The body (10) of the ultra-torr fitting is an integral part of the goniometer head and replaces one of the original translation stages. This cell requires the complete machining of the translation stage integral with the fitting and is therefore more costly than the standard cell described above. The  $O$  ring (11), grommet (12) and cap (13) are identical to those in the standard cell and the capillaries (14) are sealed in the same manner. This cell has design features

similar to those in a previously reported pressurization cell (Schiltz, Prange & Fourme, 1994) in that it uses an integrated seal within the goniometer head. However, a significant difference is that the previously designed cell utilized a Swagelok fitting that required cutting and shortening of the X-ray capillary, as well as sealing of the modified capillary in a copper sheath with epoxy. The current design requires no capillary modifications or manipulations.

### 3. Automated system for preparing xenon derivatives at SSRL beamline 7-1

A schematic diagram of the automated xenon pressure system is shown in Fig. 2. A high-capacity gas tank (17) (Spectra Gases Inc., Vista, CA, USA) is regulated at a pressure of approximately 2 MPa with a regulator (18) (Valin, Sunnyvale, CA, USA) equipped with a pressure-relief valve set to burst at a pressure of just over 2 MPa. An in-line automatic excess flow valve (19) (Sunnyvale Valve and Fitting Company) prevents gas from being wasted should a leak develop in the system. The components are connected via  $\frac{1}{8}$  in-diameter stainless-steel tubing (20) (Valin) and standard  $\frac{1}{8}$  in Swagelok fittings (21) (Sunnyvale Valve and Fitting Company). The pressure is further regulated in parallel by two pressure regulators (22) (Valin), one permanently set at 0.3 MPa and the other adjustable up to 2 MPa. Complementary electronic solenoids (23) (Valin) are used to select the appropriate pressure line. Needle valves (24) (Sunnyvale Valve and Fitting Company) are used to decrease the flow rate so that automatic filling does not produce a shock wave in the capillary. The distance between the solenoid valves and the pressure cell is kept short, to minimize waste of gas during the pressurize-vent cycle. A pressure transducer (25) (Omega, Stamford, CT, USA) measures the pressure of the cell and the value is displayed digitally (26) (Omega). A third solenoid (27) is used for automatic venting of the pressure cell. A quick-disconnect connector (28) (Sunnyvale Valve and Fitting Company) allows easy removal of the cell and goniometer head (29) from the system. The gas side of the connector automatically seals and the cell side remains open to the atmosphere when disconnected. A  $\frac{1}{8}$  in-diameter flexible Teflon gas-delivery tube (30) is used between the quick-disconnect connector and the pressure cell (31).

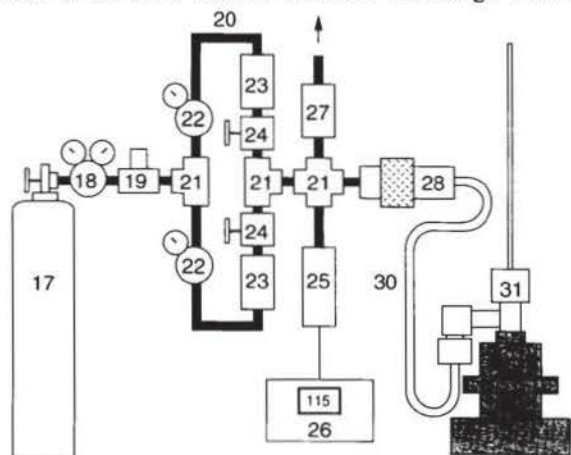


Fig. 2. Schematic diagram of the components used to build the gas delivery system: 17 gas tank; 18 high-pressure regulator; 19 excess-flow valve; 20 stainless-steel tubing; 21 Swagelok fitting; 22 pressure regulator; 23 electric solenoid; 24 needle valve; 25 pressure transducer; 26 pressure readout; 27 electric solenoid; 28 quick disconnect; 29 goniometer head; 30 flexible tubing; 31 pressure cell.

### 4. Operation

The operation of the pressure cell involves the following three basic steps: placement of the X-ray capillary with a mounted crystal in the ultra-torr fitting, several pressurization-vent



Table 2. *Observed glass and quartz capillary failure pressures in MPa*

The capillaries have a length of 9 cm and a wall thickness of 0.01 mm. The recommended maximum pressures are shown in parentheses.

Diameter (mm)				
0.3	0.5	0.7	1.0	1.5
>10*	>10*	>10*	4.5–5.0 (4.0)	4.0–4.5 (3.5)

Maximum pressure tested

cycles, and equilibration. A standard closed-end capillary, without visible defects, should be used for mounting of a sample crystal. Modest absorption problems can occur for pressure ranges above 2 MPa and large-diameter capillaries (see Table 1). It is, therefore, important that the diameter of the crystal and the diameter of the capillary are carefully matched in order to minimize such effects. A sliver of wet filter paper can be inserted in the open end of the capillary to prevent the crystal from drying out; however, special care should be taken to ensure that there is no blockage in the capillary. The capillary is installed by first being inserted into the body of the ultra-torr fitting (1). The O ring (2) is placed around the capillary and is allowed to rest on the flared portion of the capillary. It is important to ensure that the O ring is free from particulates for a proper seal. The sealing grommet (3) follows next and rests on the O ring. The ultra-torr cap (4) is placed over the capillary. The pressure cell seals properly when the cap is finger-tight.

The pressure cell can be simply connected to a gas tank via flexible Teflon tubing with an in-line three-way valve for venting to the atmosphere. **Caution: wear eye protection and protect sensitive detector equipment during the pressurization of the cell.** The result of capillary failure is complete disintegration of the X-ray capillary; appropriate precautions for both personnel and equipment should be taken. Table 2 lists a variety of capillary sizes and their observed failure pressures in MPa. Owing to the cost of xenon gas, it is advised that for higher-pressure experiments in which xenon will be used (>2 MPa), capillaries should be tested with nitrogen gas prior to mounting of the crystal. The cell is purged by the performance of several pressurization–vent cycles at a pressure of 0.3 MPa. Subsequently, the cell is brought to the desired pressure in a stepwise fashion by opening and closing of the main tank valve followed by raising of the pressure with the regulator valve. This procedure ensures against complete venting of the tank in the event of capillary failure. A slight modification has allowed us to use this system with crystals of oxygen-sensitive proteins such as ORF2 (Table 3). By the placing of a second valve between the cell and the purge valve, a crystal can be mounted in the cell in an anaerobic chamber and sealed. The air trapped in the gas line can be purged in a manner similar to that described above and finally the cell is equilibrated with gas. After the sample is allowed to equilibrate at the desired pressure, data collection can begin. Schiltz, Prange & Fourme (1994) estimate xenon gas diffuses into protein crystals in less than 30 min, based on several time-resolved experiments. We typically wait about 30 min before beginning data collection.

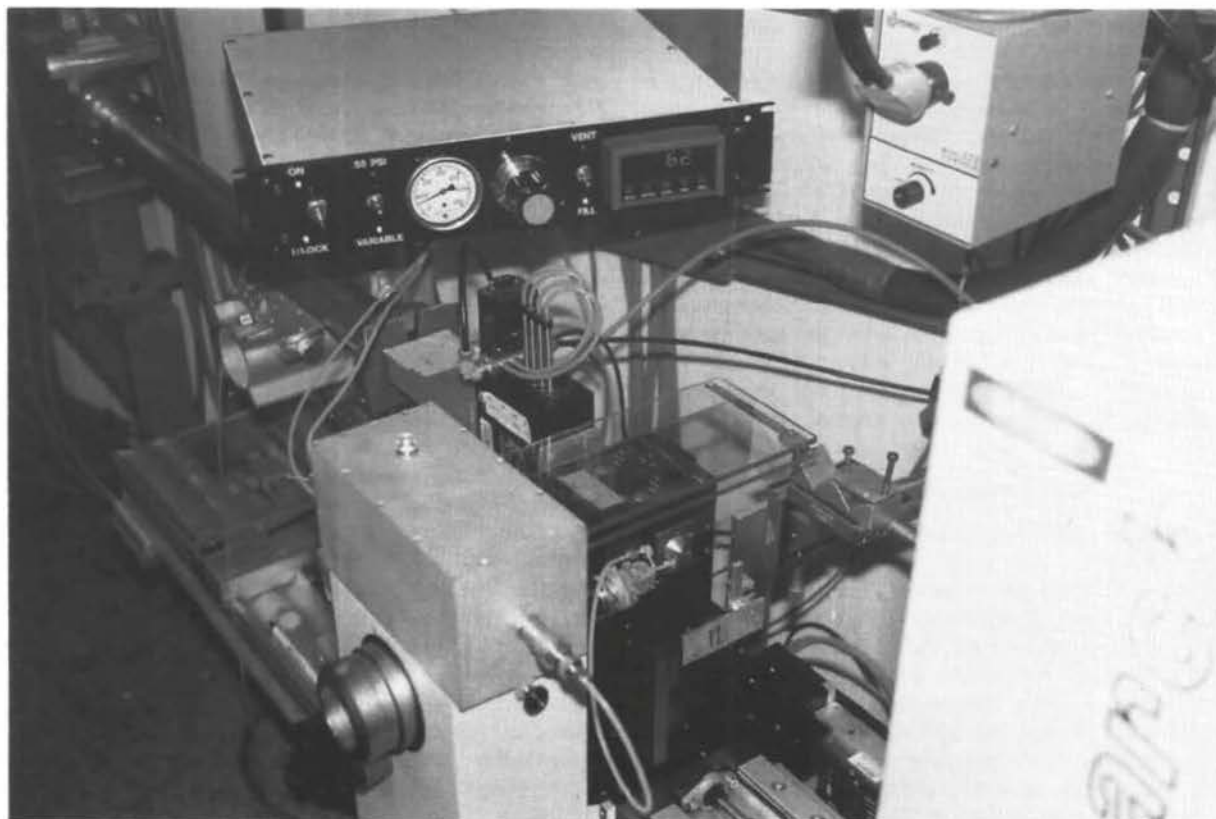


Fig. 3. Photograph of the gas-delivery system installed on beamline 7-1 at SSRL. The standard pressure cell is shown mounted on the  $\phi$  spindle of a MAR Research imaging-plate scanner system. The retractable Plexiglas shield is mounted just above the pressure cell. The control and display box (black panel) is shown mounted above the beamline components.

Table 3. Protein crystal derivatization using xenon gas

Protein	Molecular weight (kDa)	Xenon pressure (MPa)	Patterson	Difference Fourier	Number of sites	Unique site	Reference
BPI	50	1		Yes	4	Yes	(a)
CAM	23	0.4–1	Noniso				(a)
CHIP	28	0.4–1	No				(a)
C554	25	1	Poor		3		(a)
DMSOR	85	1	Yes		1	Yes	(a)
HHB	67	0.3			1		(b)
HLC	25	1.2			1	Yes	(c)
IMPDH	58	0.4–1	Noniso				(a)
LYS	14	0.8	Poor		4		(c)
MBA	18	0.3		Yes	2		(d)
MB	18	0.3		Yes	1		(e)
MB	18	0.7		Yes	4		(f)
MB	18	0.7		Yes	4		(g)
ORF2	30	1.2	Yes	Yes	1	No	(a)
PPE	26	0.8	Yes		1		(c)
RXR- $\alpha$	30	2	Yes		2	Yes	(h)
SC	27	1.2		Yes	1		(i)
SOD	16	1		Yes	1	Yes	(a)
STCN	12	1		Yes	1	Yes	(a)

Abbreviations: BPI human bactericidal permeability-increasing protein; CAM carbonic anhydrase, *Methanosarcina thermophila*; CHIP human erythrocyte aquaporin; C554 cytochrome *c554*, *Nitrosomonas europaea*; DMSOR dimethyl sulfoxide reductase, *Rhodobacter sphaeroides*; HHB horse haemoglobin; HLC collagenase, *Hypoderma lineatum*; IMPDH inosine monophosphate dehydrogenase, *Tritrichomonas fetus*; ORF2 nitrogen fixation specific open reading frame 2, *Azotobacter vinelandii*; PPE porcine pancreatic elastase; RXR- $\alpha$  human retinoid-X receptor alpha; STCN stielacyanin, cucumber; MB sperm whale myoglobin; MBA alkaline sperm whale myoglobin; SC subtilisin Carlsberg, *Bacillus licheniformis*; SOD superoxide dismutase, *Saccharomyces cerevisiae*.

References: (a) This work; (b) Schoenborn (1965); (c) Schiltz, Prange & Fourme (1994); (d) Schoenborn (1969); (e) Schoenborn, Watson & Kendrew (1965); (f) Tilton, Kuntz & Petsko (1984); (g) Vitali, Robbins, Almo & Tilton (1991); (h) Bourguet, Ruff, Chambon, Gronemeyer & Moras (1995); (i) Shiltz, Prange & Fourme (1995).

We have maintained gas pressures of 2 MPa without noticeable pressure loss for as long as 48 h.

The xenon-delivery system installed at SSRL on beamline 7-1, shown in Fig. 3, is intended for users to produce xenon derivatives in a safe and easy manner. The system obviates many potential operating hazards. The pressurization–vent cycle is accomplished simply by toggling of a switch on a control panel. The final pressure, digitally displayed, can be selected by the user via a regulator valve. The system employs a quick-disconnect connector affixed to a MAR Research imaging-plate scanner; when disconnected, the pressure cell is open to the atmosphere. This ensures that experimenters cannot carry a pressurized cell away from the scanner. As an additional safety measure, a retractable Plexiglas shield incorporating safety interlocks is installed above the pressure cell.

### 5. Experimental results

The use of xenon for heavy-atom-derivative preparation and phase determination has been proposed (Schoenborn & Featherstone, 1967) and demonstrated (Vitali, Almo, Robbins & Tilton, 1991). Recently, xenon was shown to be an effective derivative for serine proteinases and related proteins (Schiltz, Prange & Fourme, 1994). We have investigated xenon-derivative formation using the pressure cell described above and the results are summarized in Table 3. Also included in this table are previously published examples of xenon-derivative formation. As can be seen, a variety of different types of proteins have been tested and the results vary quite dramatically from exceptional derivatives to nonisomorphism. The ability of xenon to form extremely isomorphous derivatives of large-molecular-weight proteins was demonstrated with dimethyl

sulfoxide reductase (DMSOR), an 85 KDa protein. X-ray data collected to 4 Å resolution from DMSOR at 1 MPa of xenon gas gave a mean fractional isomorphous difference of only 6.5%. However, the difference Patterson calculated with data between 30 and 4 Å resolution showed a single well defined xenon site with a height of 8.5 times the root-mean-square deviation of the map (Fig. 4). Phasing statistics from this derivative were of good quality (Table 4). Another example is the nitrogen fixation specific open reading frame 2 protein (ORF2), where the observed xenon site gave superior phasing statistics in comparison to five other heavy-atom derivatives and was essential in obtaining an interpretable electron-density map (J. W. Peters *et al.*, unpublished results).

One of the most important features of xenon derivatization is that, in the cases examined to date, the xenon site appears to be different from other heavy-atom sites. This proved to be important in the case of bactericidal permeability-increasing protein (BPI), where attempts to find further derivatives were unsuccessful owing to binding of different heavy-atom compounds at identical sites. In contrast, xenon derivatization gave new sites and provided the additional phasing information necessary to obtain interpretable electron-density maps (L. Beamer *et al.*, unpublished results). Another advantage with xenon derivatization is that the number of binding sites can, in some cases, be controlled by changing of the pressure. In the case of myoglobin, an increase in pressure from 0.3 to 0.7 MPa increases the number of binding sites from 1 to 4 (See Table 3).

Interestingly, several protein crystals showed nonisomorphism when xenon derivatization was attempted. Carbonic anhydrase (CAM) showed a greater than 2% change in cell constants at xenon pressures ranging from 0.4 to 1.0 MPa. Under similar conditions, inosine monophosphate dehydrogen-



ase (IMPDH) crystals showed dramatic cell changes resulting in complete loss of diffraction. In the case of CAM, it was observed that an equivalent pressure of nitrogen gas had no effect on crystal isomorphism and we conclude that the nonisomorphism of xenon-pressurized crystals was due to a strong binding interaction between the xenon and the protein.

### 6. Concluding remarks

The gas cell described has several distinct advantages over previously reported pressure cells and pressurization techniques: it is simple to use, inexpensive and requires no modification to either X-ray capillaries or in crystal-mounting techniques. Xenon has been shown to form highly isomorphous derivatives of native crystals. In the cases we have studied, the success rate for xenon derivatization was greater than 50%, which suggests that this method of derivatization should be tested on all new crystals in the laboratory. In most cases, the derivatization is reversible, so that one could attempt further

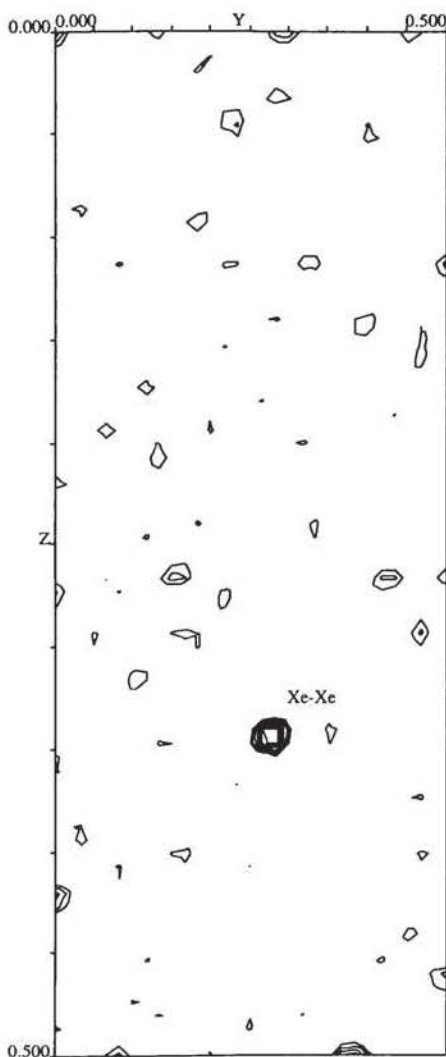


Fig. 4. Asymmetric unit of the 1 MPa xenon isomorphous difference Patterson for DMSO reductase,  $\mu = 0.5$  Harker section. The map is contoured at  $1.0\sigma$  intervals, starting at  $2.0\sigma$ . Created using the XTALVIEW2.0 software package (McRee, 1995).

Table 4. Phasing statistics for the xenon derivative of DMSO reductase

Occupancy and  $B$  refinement calculated using VECREF and phasing statistics calculated using MLPHARE of the CCP4 suite of programs (Collaborative Computational Project, Number 4, 1994).

Occupancy	0.34								
$B$	28.1								
Resolution	8.9	8.0	7.3	6.7	6.1	5.7	5.3	5.0	Total
Phasing power									
Acentric	1.23	1.34	1.09	1.10	1.08	0.98	0.94	0.89	0.92
Centric	0.54	0.89	0.69	0.95	0.75	0.73	0.69	0.59	0.65
Mean figure of merit	0.34	0.28	0.24	0.26	0.25	0.22	0.19	0.16	0.24

heavy-atom soaks on the same crystal, if xenon did not show promising results. Furthermore, xenon derivatives in general appear to give unique binding sites.

An obvious extension of this method is to use krypton in place of xenon. Krypton has a conveniently located absorption edge near 14 keV and should allow enhanced anomalous and MAD (multiple anomalous scattering) experiments to be performed under krypton pressure at synchrotron sources. With the availability of third-generation synchrotron sources, even the high-energy (34.6 keV)  $K$  absorption edge of xenon may be accessible for MAD data collection in the near future.

Finally, while the preparation of isomorphous xenon heavy-atom derivatives is an important use of the pressure cell described in this contribution, there are other important applications for such a pressure cell, including the study of protein reactions with gaseous substrates and/or inhibitors.

This work was supported in part by NIH GM45062 of the NSF to DCR and by the DOE, Office of Basic Energy Sciences and the Office of Health and Environmental Research, and by the NIH, Biomedical Research Technology Program, National Center for Research Resources for support of the rotation-camera facilities at SSRL. JPH is supported by a DOE Alexander Hollaender Distinguished Postdoctoral Fellowship. We wish to thank R. P. Phizackerley for assistance in the design of the gas-delivery system and Hartmut Luecke and Henry D. Bellamy for helpful discussions.

### References

- Bourguet, W., Ruff, M., Chambon, P., Gronemeyer, H. & Moras, D. (1995). *Nature (London)*, **375**, 377–382.
- Collaborative Computational Project, Number 4 (1994). *Acta Cryst. D50*, 760–763.
- Kroeger, K. S. & Kundrot, C. E. (1994). *J. Appl. Cryst.* **27**, 609–612.
- McRee, D. (1995). *XTALVIEW2.0: Macromolecular Crystallographic Package*. The Scripps Research Institute, La Jolla, CA, USA.
- Schiltz, M., Prange, T. & Fourme, R. (1994). *J. Appl. Cryst.* **27**, 950–960.
- Schiltz, M., Prange, T. & Fourme, R. (1995). *Structure*, **3**, 309–316.
- Schoenborn, B. P. & Featherstone, R. M. (1967). *Adv. Pharmacol.* **5**, 1–17.
- Schoenborn, B. P. (1965). *Nature (London)*, **208**, 760–762.
- Schoenborn, B. P. (1969). *J. Mol. Biol.* **45**, 297–303.
- Schoenborn, B. P., Watson, H. C. & Kendrew, J. C. (1965). *Nature (London)*, **207**, 28–30.
- Tilton, R. F., Kuntz, I. D. & Petsko, O. A. (1984). *Biochemistry*, **23**, 2849–2857.
- Vitali, J., Robbins, A. H., Almo, S. C. & Tilton, R. F. (1991). *J. Appl. Cryst.* **24**, 931–935.